
Continuous Object Representation Networks: Novel View Synthesis without Target View Supervision

Nicolai Häni Selim Engin Jun-Jee Chao Volkan Isler
 $\{\text{haeni001, engin003, chao0107, isler}\}@umn.edu$
 University of Minnesota

Abstract

Novel View Synthesis (NVS) is concerned with synthesizing views under camera viewpoint transformations from one or multiple input images. NVS requires explicit reasoning about 3D object structure and unseen parts of the scene to synthesize convincing results. As a result, current approaches typically rely on supervised training with either ground truth 3D models or multiple target images. We propose Continuous Object Representation Networks (CORN), a conditional architecture that encodes an input image’s geometry and appearance that map to a 3D consistent scene representation. We can train CORN with only two source images per object by combining our model with a neural renderer. A key feature of CORN is that it requires no ground truth 3D models or target view supervision. Regardless, CORN performs well on challenging tasks such as novel view synthesis and single-view 3D reconstruction and achieves performance comparable to state-of-the-art approaches that use direct supervision. For up-to-date information, data, and code, please see our project page¹.

1 Introduction

In 1971, Shephard and Metzler [44] introduced the concept of mental rotation, the ability to rotate 3D objects mentally and link the model to its projection. Novel View Synthesis (NVS) research seeks to replicate this capability in machines by generating images of a scene from previously unseen viewpoints, unlocking applications in image editing, animation, or robotic manipulation. View synthesis is a challenging problem, as it requires understanding the 3D scene structure, reason on image semantics, and the ability to render the internal representation into a target viewpoint. A common approach for NVS is to use a large collection of views to reconstruct a 3D mesh [10, 43]. Recent methods have made progress in learning 3D object representations, such as voxel grids [60, 46, 52, 33, 32], point clouds [1, 61, 56], or meshes [54, 12, 48, 55]. However, the discrete nature of these representations limit the achievable resolution and induce significant memory overhead. Continuous representations [36, 25, 42, 47, 58, 6, 24, 27] address these challenges. However, proposed methods require either 3D ground truth or multi-view supervision, limiting these approaches’ applicability to domains where data is available.

We introduce Continuous Object Representation Networks (CORNs), a neural object representation that enforces multi-view consistency in geometry and appearance with natural generalization across scenes, learned from as few as two images per object. The key idea of CORNs is to extract local and global features from the input images and represent the scene implicitly as a continuous, differentiable function that maps local and global features to 3D world coordinates. We optimize CORNs from only two source views using transformation chains and 3D feature consistency as self-supervision, requiring $50\times$ fewer data during training than the current state-of-the-art models.

¹Project page: nicolaihaeni.github.io/corn/

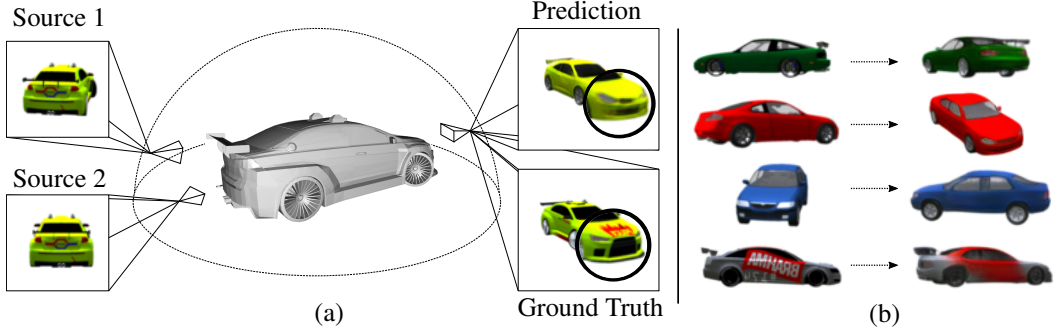


Figure 1: Our model learns to synthesize novel views using only two source images per object during training (a). For this instance, even though both source images are from the back of the car, our model can reconstruct unseen areas with a reasonable detail level. During training, the target view prediction is *not* directly supervised with ground truth. Instead, it is transformed into the second source image while maintaining the consistency of the learned representation. During inference (b), our model predicts novel views from a single input image. It can accommodate drastically different source and target poses.

The conditional formulation of CORNs, combined with a differentiable neural renderer, enforces multi-view consistency and allows for the fast inference of novel views from a single image during test time, without additional optimization of latent variables. We evaluate CORNs on various challenging 3D computer vision problems, including novel view synthesis, 3D model reconstruction, and out of domain view synthesis.

To summarize, our approach makes the following contributions:

- A continuous, conditional novel view synthesis model, CORNs based on a novel representation that captures the scene’s appearance and geometry at arbitrary spatial resolution. CORNs are end-to-end trainable and uses only two images per object during training time, without any 3D space or 2D target view supervision.
- Despite being self-supervised, CORN performs competitively or even outperforms current state-of-the-art approaches that use dozens of images per object and direct supervision on the target views.
- We demonstrate several applications of our method, including novel view synthesis, single-view 3D reconstruction, and novel view synthesis from out-of-domain samples.

2 Related Work

Our goal is to generate novel camera perspectives of static 3D scenes. As such, our work lies at the intersection of novel view synthesis, 3D object reconstruction, and generative modeling. In the following, we review related work in these areas.

Novel view synthesis. Novel view synthesis is the problem of generating new camera perspectives of a scene. Key challenges of novel view synthesis are inferring the scene’s 3D structure and inpainting occluded and unseen parts. Existing methods differ in their generality, some aim to learn a general model for a class of objects [59, 33, 5, 47], while others learn instance-specific models [46, 26, 28]. Training an instance-specific model generally produces higher quality results, at the cost of lengthy training times for each object instance. For real-world applications, this is often prohibitive. Improving general models is an open problem, and as CORNs generalize naturally across object instances, we focus our literature review on methods that synthesize novel views for a general category of objects.

Traditionally, novel view synthesis uses multi-view geometry [7, 10, 43] to triangulate 3D scene content. Once the 3D scene is reconstructed, novel views can be generated by rendering the resulting 3D mesh. Instead of explicit 3D mesh reconstruction, other approaches have sought to represent 3D knowledge implicitly; by directly regressing pixels in the target image [50, 49, 59], weakly disentangling view pose and appearance [67, 62, 22] or by learning appearance flow [65, 35, 49, 5].

Other prior work proposed to apply the view transformations in latent space [57] or learn a complete latent space of posed objects [51] from which to sample. While these techniques successfully predict novel views under small viewpoint transformations, they do not allow 3D structure extraction. Our proposed method encapsulates both the scenes 3D structure and appearance and can be trained end-to-end via a differentiable renderer.

Neural scene representations. Deep-learning-based image rendering has become an active research area, creating a plethora of geometric proxy representations. Broadly, these representations can be categorized on whether they represent 3D geometry implicitly or explicitly. Explicit representations include voxels [60, 46, 52, 33, 32], meshes [54, 12, 48, 55] or point clouds [1, 61, 56]. While these discretization based methods have enabled some impressive results, they are memory intensive and limited in the representation of complicated surfaces. To improve upon these shortcomings, recent work focuses on learning neural scene representations. Generative Query Networks (GQN) (GQN) [9, 23, 31] a framework to learn low dimensional embedding vectors that represent both the 3D scenes structure and appearance. While GQNs allow sampling of 2D view samples consistent with its lower-dimensional embedding, they disregard the scenes 3D structure.

Continuous function representations represent 3D space as the level set of a function, parametrized by a memory-efficient neural network, which can be sampled to extract 3D structure. Different function representations have emerged, such as binary occupancy classifiers [6, 24, 27], signed distance functions [36, 25, 42, 47, 58] or volumetric representations [28]. While these techniques are successful at modeling 3D geometry, they often require 3D supervision. When combined with a differentiable renderer, some approaches are supervised with 2D target images instead, relying on large image collections for training. However, it can be difficult for real-world applications to obtain dozens or even hundreds of images of each object we would like to model. In contrast, our proposed method encapsulates scene geometry and appearance from *only two reference images per object* and can be trained end-to-end via a learned neural rendering function through self-supervision.

Generative models. Our work builds on recent advances in generating high-quality images with deep neural networks. Especially Generative Adversarial Networks (GAN) [13, 38, 3] and its conditional variants [30, 16, 66] have achieved photo-realistic image generation. Some approaches synthesize new views by incorporating explicit spatial or perspective transformations into the network [15, 17, 60]. Another approach is to treat novel view synthesis as an inverse graphics problem [22, 62, 21, 53, 45, 63]. However, these 2D generative models only learn to parametrize 2D views and their respective transformations and struggle to produce multi-view consistent outputs since the underlying 3D structure cannot be exploited.

3 Method

Given a dataset $\mathcal{D} = \{(I_{1,2}^i, K_{1,2}^i, T_{1,2}^i)\}_{i=1}^N$ of N objects, each consisting of a tuple with two images $I_{1,2}^i \in \mathbb{R}^{H \times W \times 3}$ and their respective intrinsic $K_{1,2}^i \in \mathbb{R}^{3 \times 3}$ and extrinsic $T_{1,2}^i \in \mathbb{R}^{3 \times 4}$ camera matrices, our goal is to learn a function f that synthesizes novel views at arbitrary goal camera poses $T_G^i \in \mathbb{R}^{3 \times 4}$ (Fig. 2). We parametrize $f = f_\theta$ as a neural network with parameters θ that naturally enforces 3D structure and enables generalization of shape and appearance across objects. We are interested in a conditional formulation of f_θ that requires no additional optimization of latent variables at inference time, and that can be optimized from only two images per object. In the following, we first introduce the three components of our network and then discuss how to optimize with limited data from only two input images per object. For notational simplicity, we drop the superscript denoting the specific object.

3.1 Feature encoding

The feature encoder network e maps input images to a lower-dimensional feature encoding. Inspired by Xu et al. [58], we hypothesize that combining a global feature encoding with spatial pixel-wise features increases the level of detail of the generated images, which we confirm in Sec. 4. The global encoder predicts a global feature vector z that should represent object characteristics such as geometry and appearance. The spatial feature encoder predicts feature maps at the same resolution as the input image. Sampling from this feature map should represent scene semantics beyond merely RGB color and provide additional details to the 3D scene representation.

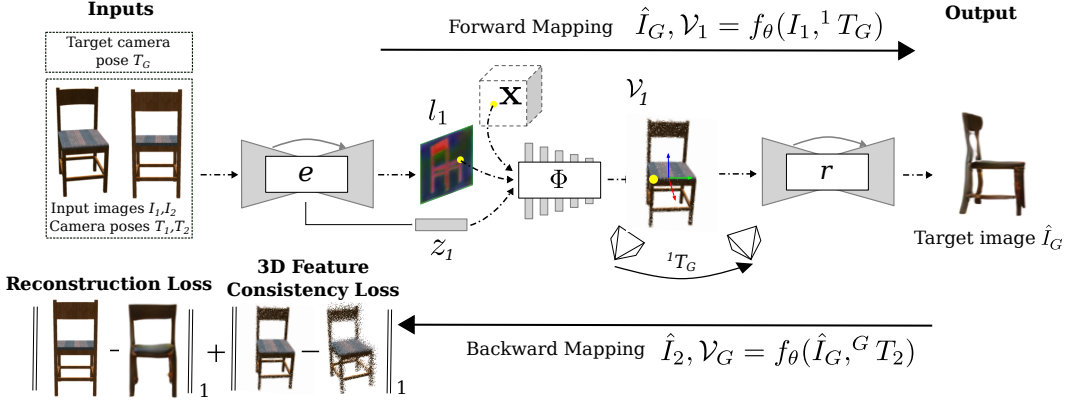


Figure 2: **Our proposed end-to-end model.** CORN takes two source images $I_{1,2}$, together with their respective camera poses $T_{1,2}$, and a target camera pose T_G as input. We aim to learn a function $\hat{I}_G = f_\theta(I_1, {}^1 T_G)$ that synthesizes novel views \hat{I}_G at target pose T_G . Our approach consists of three parts. The *feature predictor* e embeds the input image in a lower dimensional feature space (visualization by projecting features with PCA). The *neural scene representation*, Φ , maps these features to a 3D consistent neural representation in world coordinates (x, y, z) (the diagram shows RGB for clarity). Finally, a *neural renderer* r renders the scene from arbitrary novel views T_G .

Global feature encoder. To predict a global feature embedding, we use a ResNet-18 [14] network to extract a 128-dimensional global feature $z \in \mathbb{R}^{128}$. We initialize the ResNet-18 with weights pretrained on the ImageNet dataset and allow further optimization during training.

Spatial feature network. The spatial feature network builds on the UNet [40] architecture. It takes the last two-dimensional feature map of the global feature encoder as input, followed by four upsampling and skip-connection layers to extract a 64-dimensional per-pixel feature $l \in \mathbb{R}^{64 \times H \times W}$ of the same size as the input image.

3.2 Neural scene representation

Our neural scene representation Φ maps a spatial location $\mathbf{x} \in \mathbb{R}^3$, the global object descriptor z , and local features l to a feature representation of learned scene properties at spatial location \mathbf{x} . The feature representation may encode visual information, such as RGB color, but it may also encode higher-order information, such as binary occupancy. In contrast to discrete representations, such as voxel grids or point clouds, which only sparsely sample object properties, Φ densely models object properties, which can, in theory, be sampled at arbitrary resolutions. In contrast to recent work on representing scenes as continuous functions with a single global object descriptor [36, 47] we combine global and local features. Combining local and global features is similar to recent work by Xu et al. [58] on single-view 3D model reconstruction, which has shown improved performance on modeling fine details.

Our implicit representation Φ is aware of the 3D structure of objects, as the input to Φ contains world coordinates \mathbf{x} . We sample k 3D points $\{\mathbf{x}_j\}_{j=1}^k$ uniformly at random from a cubic volume and extract local features by projecting the 3D points to the feature map l using the known camera pose. We follow a perspective pinhole camera model that is fully specified by its extrinsic $E = [R, t] \in \mathbb{R}^{3 \times 4}$ and intrinsic $K \in \mathbb{R}^{3 \times 3}$ camera matrices. The extrinsic camera matrix contains rotation matrix $R \in \mathbb{R}^{3 \times 3}$ and translation vector $t \in \mathbb{R}^3$. Given a 3D coordinate \mathbf{x}_j , the projection from world space to the camera frame is given by:

$$\mathbf{u} = [u \quad v \quad 1]^\top = K(R\mathbf{x}_j + t) \quad (1)$$

where u and v are the pixel coordinates in the image plane. We extract local features l_{uv} using bilinear sampling, which is fast to compute and differentiable. The neural representation network Φ takes concatenated global features, local features, and world coordinates $(z, l_{uv}, \mathbf{x}) \in \mathbb{R}^m$ as input and maps them to a higher dimensional feature $\mathbf{v}_j \in \mathbb{R}^n$ at the given spatial coordinate \mathbf{x}_j :

$$\Phi : \mathbb{R}^m \rightarrow \mathbb{R}^n, (z, l_{uv}, \mathbf{x}_j) \mapsto \Phi(z, l_{uv}, \mathbf{x}_j) = \mathbf{v}_j \quad (2)$$

We denote the collection of features at sampled points by $\mathcal{V} = \{\mathbf{v}_j\}_{j=1}^k$, and in our experiments use a 64-dimensional feature \mathbf{v}_j for each spatial location. We also predict occupancy probabilities for each 3D point to increase spatial consistency, which we render as binary masks. In Sec. 4, we show that this formulation leads to multi-view consistent novel view synthesis results.

3.3 Point encoding

Instead of operating on (x, y, z) world-coordinates directly, we found that learning a higher dimensional embedding of the 3D space improves the overall performance. This is consistent with recent work [39, 29], which show that neural networks are biased towards learning low frequency functions. A higher dimensional encoding of world-coordinates can increase the network’s capacity to model high-frequency details. Previous works also showed, that using deterministic trigonometric functions for the point encoding γ achieves similar performance as when γ is parametrized as an MLP. Following Mildenhall et al. [29] we parametrize γ as non-learned composition of trigonometric functions:

$$\gamma(\mathbf{x}) = (\sin(2^0\pi\mathbf{x}), \cos(2^0\pi\mathbf{x}), \dots, \sin(2^{L-1}\pi\mathbf{x}), \cos(2^{L-1}\pi\mathbf{x})). \quad (3)$$

In our experiments, we set $L = 10$ and apply γ to each point coordinate individually.

3.4 Neural renderer

Given a 3D feature space \mathcal{V} of a scene sampled at 3D points, we introduce a neural rendering algorithm that maps a 3D feature space \mathcal{V} as well as the intrinsic K and extrinsic camera parameters T to a novel view \hat{I}_G target camera pose T_G . The sampled feature points are projected to the image plane at the target camera’s transformation matrix T_G high-performance renderer based on [56]. The neural renderer projects a 3D feature point \mathbf{v}_j to a region in image space with center c_j , and radius r , where the features influence on a given pixel p_{uv} is given by it’s Euclidean distance d to the region’s center:

$$p_{mn} = \begin{cases} \mathcal{N}(\mathbf{v}_j, p_{uv}) = 0 & \text{if } d(c_j, p_{uv}) > r \\ \mathcal{N}(\mathbf{v}_j, p_{uv}) = 1 - \frac{d(c_j, p_{uv})}{M} & \text{otherwise} \end{cases} \quad (4)$$

where r and M are controllable hyper-parameters. Although \mathcal{N} is non-differentiable, Wiles et al. [56] approximate derivatives using the sub-derivative. The projected points are accumulated in a z-buffer and sorted according to the distance from the new camera before accumulating into a projected feature map $\bar{\mathcal{V}} \in \mathbb{R}^{64 \times H \times W}$ using alpha over-compositing. For additional technical details, please refer to the excellent description in [56].

To render the high dimensional projected features into an RGB image, we use a refinement network r . The refinement network renders color values, infers missing features, and reasons for the image’s occluded regions. The refinement network is built on a UNet [40] architecture with four down/upsampling blocks and skip connections and spectral normalization [39] following each convolution layer to regularize training.

3.5 Training details

To discover a meaningful 3D scene representation without 3D or 2D target image supervision, we assume without loss of generality that for an object, there exists a unique 3D object representation in a canonical view frame. We define the objects’ frontal view (0° azimuth and 0° elevation) as the canonical view. To learn such a canonical 3D representation, we offer two key insights: 1) If at least two source images per object are available, we can use transformation chains as supervision, and 2) for the same object, the sampled 3D feature space \mathcal{V} has to be multi-view consistent. In the following, we introduce two loss terms that enforce these insights.

Transformation chain loss. Given two source images, I_1 and I_2 of an object, we learn a multi-view consistent 3D feature space through transformation chains. We define a transformation chain as:

$$\hat{I}_2 = f_\theta(f_\theta(I_1, {}^1T_G,)^G T_2) \quad (5)$$

where we first transform source image I_1 with relative transformation 1T_G from camera pose T_1 to T_G and subsequently transform the intermediate prediction \hat{I}_G with relative transformation ${}^G T_2$. Similarly, we transform source view I_2 to camera pose T_1 . To additionally regularize the

network output, we add supervision by transforming the source views to their respective camera pose: $\bar{I}_2 = f_\theta(I_1, {}^1T_2)$ and $\bar{I}_1 = f_\theta(I_2, {}^2T_1)$. We use a combination of L_1 and perceptual losses [18] to get our transformation loss

$$\mathcal{L}_{\text{trafo}}(f_\theta, I_{1,2}, T_{1,2}, T_G) = \sum_{i \in \{1,2\}} ||I_i - \hat{I}_i||_1 + ||I_i - \bar{I}_i||_1 + ||I_i - \hat{I}_i||_{\text{vgg}} + ||I_i - \bar{I}_i||_{\text{vgg}}. \quad (6)$$

3D feature consistency loss. We assume the object to be in a canonical view frame which allows us to enforce 3D feature consistency among transformation chains. We define 0° for azimuth and elevation as our canonical camera frame. To enable comparison across transformation chain, 3D points \mathbf{x} are sampled at the beginning of each iteration. Given the sampled 3D feature spaces ${}^j\mathcal{V}_i$ of all transformation chains, we enforce feature space consistency with

$$\mathcal{L}_{\text{3d}}(f_\theta, I_{1,2}, T_{1,2}, T_G) = \sum_{i \neq j} ||\mathcal{V}_j - \mathcal{V}_i||_1 \quad (7)$$

for $i, j \in \{1, 2, G\}$.

Other losses. To encourage the network to generate spatially meaningful features in 3D space, we also use our object representation network Φ to predict occupancy for the sampled 3D points. We supervise occupancy prediction using binary cross-entropy between the source masks (we segment the input image instead of using ground truth masks) and the predicted masks. Finally, to encourage the generator to synthesize realistic images, we use a GAN loss \mathcal{L}_{GAN} with a patch discriminator [16]. Our full objective function is:

$$\mathcal{L} = \lambda_{\text{trafo}} \mathcal{L}_{\text{trafo}} + \lambda_{\text{3d}} \mathcal{L}_{\text{3d}} + \lambda_{\text{BCE}} \mathcal{L}_{\text{BCE}} + \lambda_{\text{GAN}} \mathcal{L}_{\text{GAN}} \quad (8)$$

where the λ parameters are the respective weight of the loss terms.

4 Experiments

We evaluate CORN on the task of novel view synthesis for several object classes and on potential applications, namely single-view 3D reconstruction and out of distribution view synthesis on real data. For additional results, we refer the reader to the supplementary document.

Implementation details. Hyper-parameters, full network architectures for CORNs, and all baseline descriptions can be found in the supplementary material. Training of the presented models takes on the order of 2 days. Links to code and datasets are available on our project website.

4.1 Datasets

ShapeNet v2. For novel view synthesis, we follow established evaluation protocols [35, 49] and evaluate on the car and chair classes of ShapeNet v2.0 [4]. The rendered dataset contains 108 images at a resolution of 128×128 pixels per object, with camera poses sampled from a viewing hemisphere with equally spaced azimuth (ranging between $0^\circ - 360^\circ$) and elevation ($0^\circ - 20^\circ$) angles in 10-degree intervals. Of the 108 rendered images for each object, we select only two images

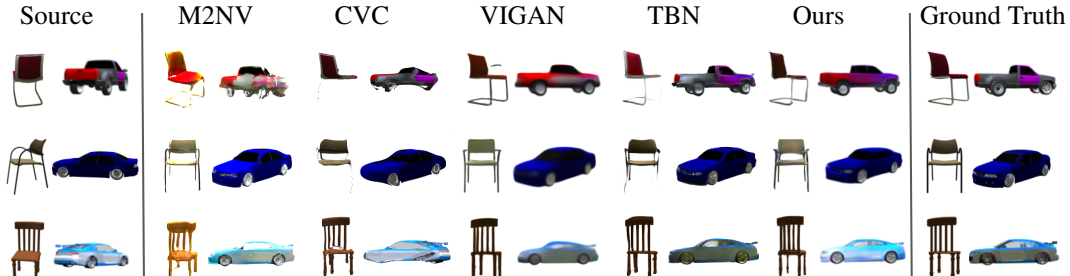


Figure 3: **Qualitative novel view synthesis results.** Our method generates detailed novel views, performing competitively to the baselines. Appearance flow methods fail to generate convincing images for large viewpoint transformations (e.g. top row of M2NV and CVC).

at random per object for CORN training. We evaluate the performance of novel view synthesis on 20,000 randomly generated test pairs of objects in the held-out test dataset. We compare CORN to four baseline methods from recent literature based on three evaluation metrics: 1) L_1 distance, 2) structural similarity (SSIM) between the predicted and ground truth images, and 3) learned perceptual image patch similarity (LPIPS) [64], a metric that better replicates human judgment of visual quality.

Basel Face Model. We show qualitative results on the Basel Face Model [11] with face models showing a range of expressions. We generate 33 renderings each from 10,000 face models with camera poses sampled from a hemisphere in front of the face with azimuth angles ranging between ($\pm 50^\circ$) and elevation ($\pm 20^\circ$). Appearance and expression parameters are sampled from a zero-mean Gaussian distribution with a standard deviation of 0.7. We use constant ambient illumination and a variation of expression and appearance parameters. After training, we evaluate our model on a holdout test set. CORNs capture the appearance and orientation of the face model and expression parameters, as seen in Fig. 4. As expected, due to the deterministic implementation, CORNs reconstructs objects resembling the mean of all feasible objects, decreasing performance for instances showing considerable divergence from the mean shape. For additional results, see the supplementary material and the video.

4.2 Results

Novel view synthesis. We evaluate our network on the task of transforming a single source-view into a target camera view. Table 1 and Fig. 3 show quantitative and qualitative results respectively. Despite using no 3D or 2D target view supervision and only two source images for training, our method performs competitively (up to within 2% of the best score) or even outperforms other methods on the LPIPS score against the supervised approaches, demonstrating CORN ability to generate meaningful object representations from a fraction of the data. The appearance flow-based methods fail if the viewpoint transformations are large (top row). Our model qualitatively preserves fine details and generates meaningful results for missing parts of the object. Using the two source images for direct supervision (CORN w 2VS) without learning a consistent 3D representation and using transformation chains decreases model performance. Similarly, relying solely on a global object description vector (CORN global) decreases performance. For additional ablations of individual loss function terms, please see the supplementary material.

Table 1: **Quantitative novel view synthesis results.** We report mean and standard deviation of the L_1 loss (lower is better), structural similarity (SSIM) index (higher is better) and learned perceptual image patch similarity (LPIPS) (lower is better) for several methods. Our model achieves competitive results, using $50\times$ less data and only two input images per object for self-supervision.

Methods	Car			Chair		
	$L_1(\downarrow)$	SSIM (\uparrow)	LPIPS (\downarrow)	$L_1(\downarrow)$	SSIM (\uparrow)	LPIPS (\downarrow)
M2NV [49]	0.139	0.751	0.238	0.114	0.738	0.217
CVC [5]	0.091	0.802	0.149	0.124	0.741	0.207
VIGAN [59]	0.0524	0.860	0.130	0.121	0.746	0.161
TBN [33]	0.0578	0.856	0.095	0.092	0.792	0.138
CORN w 2VS	0.073	0.819	0.120	0.157	0.689	0.245
CORN global	0.069	0.827	0.109	0.157	0.703	0.216
CORN	0.063	0.838	0.094	0.132	0.722	0.180

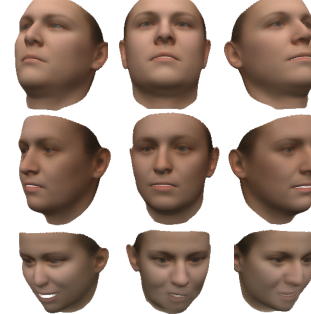


Figure 4: **Qualitative results on the Basel Face dataset.**

Continuous scene representation. We compare our method against SRN [47], a state-of-the-art continuous scene representation network. To allow a fair comparison, we use only objects at the intersection of the two evaluation protocols. We use a single source image for both models to



Figure 5: **Quantitative results of view sequence generation.** We used a single image to predict 108 target views. Our model synthesizes images with a higher level of detail, models transient object properties, and shows better form fit.

reconstruct the scene representation before generating 108 views (ranging between azimuth $0^\circ - 360^\circ$ and elevation $0^\circ - 20^\circ$ angles).

Table 2 and Fig. 5 show the qualitative and quantitative results respectively. Our method outperforms SRN, even without target view supervision, using only two images per object, compared to 50 for SRN. Our model does not require latent code optimization during inference, which dramatically reduces the inference time from about 5 minutes (SRN) to milliseconds per image.

Table 2: **Continuous representation results.** We evaluate the ability of SRN [47] and CORN to synthesize 108 novel views from a single input image on car and chair objects. Our method outperforms SRN on both datasets.

Methods	Car			Chair		
	$L_1(\downarrow)$	SSIM (\uparrow)	LPIPS (\downarrow)	$L_1(\downarrow)$	SSIM (\uparrow)	LPIPS (\downarrow)
SRN [47]	0.090	0.797	0.144	0.160	0.708	0.232
CORN	0.067	0.831	0.103	0.1333	0.725	0.181

4.3 Applications

Out of domain view synthesis. Results reported so far are on synthetic datasets where the input images are rendered from 3D CAD models. To test the generalization performance of CORNs to real data, we evaluate our model trained with the ShapeNet car objects on the Cars [19] dataset. This dataset contains a wide variety of real car images taken from natural scenes. Note that we did not retrain our model on this dataset. Fig. 6 shows the novel view synthesis of objects given real input images as input. Our method preserves local geometric and photometric features in this challenging setup. This experiment suggests that our model can synthesize images from different dataset distributions, indicating some domain transfer capability.

Single-view 3D reconstruction. In addition to novel view synthesis, our method’s possible applications include single-image 3D reconstruction. We synthesize N novel views on the viewing hemisphere from a single image. From these images, we sample k 3D points uniformly at random from a cubic volume in a similar procedure to the one described in Section 3.2. Our goal is to predict the occupancy of each of these k points. To accomplish this, we project each point onto the synthesized images and label it as occupied if it projects to the foreground mask. Fig. 7 shows the 3D reconstruction results from the input images. Our method captures the overall structure of the



Figure 6: **Qualitative results of novel view synthesis on real data.** Our model generates high quality views of previously unseen data. We use the model trained on ShapeNet and evaluate on the Cars [19] without retraining.

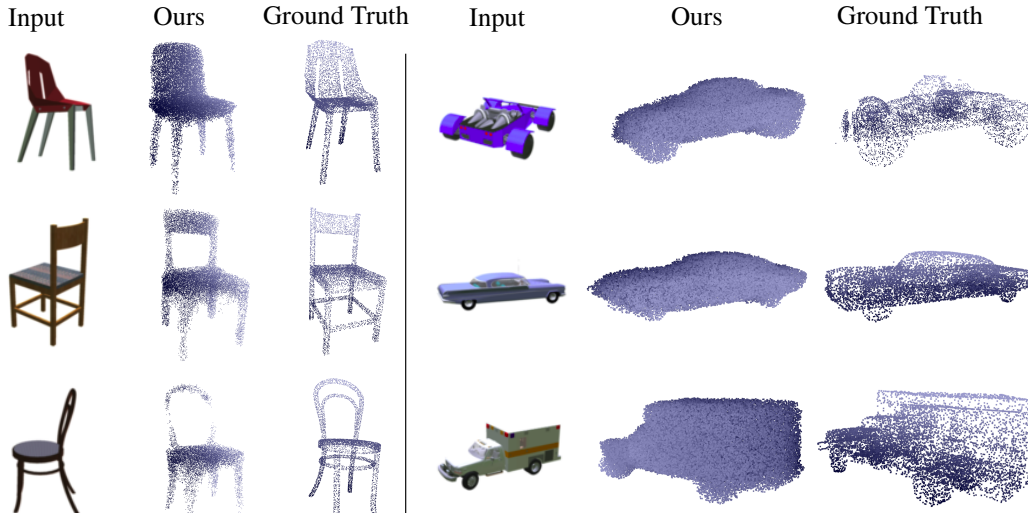


Figure 7: **Qualitative single view 3D reconstruction results.** The synthesized views can be used to produce high quality 3D reconstructions from a single input image.

objects, and in most cases, their fine-level details. In our experiments we synthesize $N = 15$ images and sample $k = 10^5$ points in 3D space.

5 Discussion

We introduced CORNs, a continuous neural representation for novel view synthesis, learned without any 3D object information or 2D target view supervision. Our system’s key component is the use of transformation chains and 3D feature consistency to self-supervise the network. The resulting continuous representation network maps local and global features, extracted from a single input image to a spatial feature representation of the scene. Incorporating a differentiable neural renderer enables the synthesis of new images from arbitrary views in an end-to-end trainable fashion. CORN requires only two source images per object during training and achieves comparable results or outperforms state-of-the-art supervised models with $50\times$ fewer data and without target view supervision. We demonstrate our model’s applications for novel view synthesis, single image 3D object reconstruction, and out of distribution view synthesis on real images.

There are several exciting possible avenues for future work. Using two input views during training to regularize the 3D representation by imposing consistency across the input training images is critical to our method’s success. We intend to investigate whether such regularization can be achieved with only one training image per object. However, the naive solution of using CORN with only a single image fails, as cyclic consistency collapses the model to the trivial solution (the identity mapping). Currently, CORNs achieve high confidence predictions from two randomly chosen training images. Sampling views more intelligently, i.e., across aspect graph [8] event boundaries could improve performance. Finally, CORN operate on synthetic data, without natural backgrounds, and with defined camera poses. Future work may alternatively integrate CORN with pose estimation and background modeling models.

Broader Impact

Our approach to learning novel view synthesis has the immediate possibility of enabling augmented and virtual reality applications [37, 20]. The limited requirement of only two images per object will make these techniques applicable beyond synthetic data. As with any generative model that provides tools for image manipulation, we too run the risk of producing fake visual content that can be exploited for malicious causes. While visual object rotation itself does not have direct negative consequences, the mere fact that such manipulations are possible can erode the public’s trust in published images [34]. Image manipulation is not a new phenomenon, however, and there has been research trying to detect manipulated images [41, 2] automatically. Still, more work on and broader adoption of such techniques is needed to mitigate image manipulation’s adverse effects.

Acknowledgments and Disclosure of Funding

Funding provided in direct support of this work came from the UMII MnDrive Graduate Assistantship Award a LCCMR grant and NSF grant 1617718. The authors acknowledge the Minnesota Supercomputing Institute (MSI) at the University of Minnesota for providing resources that contributed to the research results reported within this paper. URL: <http://www.msi.umn.edu>

References

- [1] P. Achlioptas, O. Diamanti, I. Mitliagkas, and L. Guibas. Learning Representations and Generative Models for 3D Point Clouds. In *International Conference on Machine Learning*, pages 40–49, 2018.
- [2] M. Barni, E. Nowroozi, B. Tondi, and B. Zhang. Effectiveness of random deep feature selection for securing image manipulation detectors against adversarial examples. In *IEEE International Conference on Acoustics, Speech and Signal Processing*, pages 2977–2981. IEEE, 2020.
- [3] A. Brock, J. Donahue, and K. Simonyan. Large Scale GAN Training for High Fidelity Natural Image Synthesis. In *International Conference on Learning Representations*, 2018.
- [4] A. X. Chang, T. Funkhouser, L. Guibas, P. Hanrahan, Q. Huang, Z. Li, S. Savarese, M. Savva, S. Song, H. Su, and others. Shapenet: An information-rich 3d model repository. *arXiv preprint arXiv:1512.03012*, 2015.
- [5] X. Chen, J. Song, and O. Hilliges. Monocular neural image based rendering with continuous view control. In *Proceedings of the IEEE International Conference on Computer Vision*, pages 4090–4100, 2019.
- [6] Z. Chen and H. Zhang. Learning implicit fields for generative shape modeling. In *Proceedings of the IEEE Conference on Computer Vision and Pattern Recognition*, pages 5939–5948, 2019.
- [7] P. E. Debevec, C. J. Taylor, and J. Malik. Modeling and rendering architecture from photographs: A hybrid geometry-and image-based approach. In *Proceedings of the 23rd annual conference on Computer graphics and interactive techniques*, pages 11–20, 1996.
- [8] D. Eggert, L. Stark, and K. Bowyer. Aspect graphs and their use in object recognition. *Annals of Mathematics and artificial Intelligence*, 13(3-4):347–375, 1995.
- [9] S. A. Eslami, D. J. Rezende, F. Besse, F. Viola, A. S. Morcos, M. Garnelo, A. Ruderman, A. A. Rusu, I. Danihelka, K. Gregor, and others. Neural scene representation and rendering. *Science*, 360(6394):1204–1210, 2018.
- [10] A. Fitzgibbon, Y. Wexler, and A. Zisserman. Image-based rendering using image-based priors. *International Journal of Computer Vision*, 63(2):141–151, 2005.
- [11] T. Gerig, A. Morel-Forster, C. Blumer, B. Egger, M. Luthi, S. Schönborn, and T. Vetter. Morphable face models—an open framework. In *2018 13th IEEE International Conference on Automatic Face & Gesture Recognition*, pages 75–82. IEEE, 2018.

- [12] G. Gkioxari, J. Malik, and J. Johnson. Mesh r-cnn. In *Proceedings of the IEEE International Conference on Computer Vision*, pages 9785–9795, 2019.
- [13] I. Goodfellow, J. Pouget-Abadie, M. Mirza, B. Xu, D. Warde-Farley, S. Ozair, A. Courville, and Y. Bengio. Generative adversarial nets. In *Advances in Neural Information Processing Systems*, pages 2672–2680, 2014.
- [14] K. He, X. Zhang, S. Ren, and J. Sun. Deep residual learning for image recognition. In *Proceedings of the IEEE Conference on Computer Vision and Pattern Recognition*, pages 770–778, 2016.
- [15] G. E. Hinton, A. Krizhevsky, and S. D. Wang. Transforming auto-encoders. In *International conference on artificial neural networks*, pages 44–51. Springer, 2011.
- [16] P. Isola, J.-Y. Zhu, T. Zhou, and A. A. Efros. Image-to-image translation with conditional adversarial networks. In *Proceedings of the IEEE Conference on Computer Vision and Pattern Recognition*, pages 1125–1134, 2017.
- [17] M. Jaderberg, K. Simonyan, A. Zisserman, and others. Spatial transformer networks. In *Advances in Neural Information Processing Systems*, pages 2017–2025, 2015.
- [18] J. Johnson, A. Alahi, and L. Fei-Fei. Perceptual losses for real-time style transfer and super-resolution. In *Proceedings of the European Conference on Computer Vision*, pages 694–711. Springer, 2016.
- [19] J. Krause, M. Stark, J. Deng, and L. Fei-Fei. 3d object representations for fine-grained categorization. In *Proceedings of the IEEE international conference on computer vision workshops*, pages 554–561, 2013.
- [20] M. Krichenbauer, G. Yamamoto, T. Taketom, C. Sandor, and H. Kato. Augmented reality versus virtual reality for 3d object manipulation. *IEEE transactions on visualization and computer graphics*, 24(2):1038–1048, 2017.
- [21] T. D. Kulkarni, P. Kohli, J. B. Tenenbaum, and V. Mansinghka. Picture: A Probabilistic Programming Language for Scene Perception. In *Proceedings of the IEEE Conference on Computer Vision and Pattern Recognition*, pages 4390–4399, 2015.
- [22] T. D. Kulkarni, W. F. Whitney, P. Kohli, and J. Tenenbaum. Deep convolutional inverse graphics network. In *Advances in Neural Information Processing Systems*, pages 2539–2547, 2015.
- [23] A. Kumar, S. Eslami, D. J. Rezende, M. Garnelo, F. Viola, E. Lockhart, and M. Shanahan. Consistent generative query networks. *arXiv preprint arXiv:1807.02033*, 2018.
- [24] S. Liu, S. Saito, W. Chen, and H. Li. Learning to infer implicit surfaces without 3d supervision. In *Advances in Neural Information Processing Systems*, pages 8293–8304, 2019.
- [25] S. Liu, Y. Zhang, S. Peng, B. Shi, M. Pollefeys, and Z. Cui. Dist: Rendering deep implicit signed distance function with differentiable sphere tracing. In *Proceedings of the IEEE/CVF Conference on Computer Vision and Pattern Recognition*, pages 2019–2028, 2020.
- [26] S. Lombardi, T. Simon, J. Saragih, G. Schwartz, A. Lehrmann, and Y. Sheikh. Neural volumes: learning dynamic renderable volumes from images. *ACM Transactions on Graphics (TOG)*, 38(4):1–14, 2019.
- [27] L. Mescheder, M. Oechsle, M. Niemeyer, S. Nowozin, and A. Geiger. Occupancy networks: Learning 3d reconstruction in function space. In *Proceedings of the IEEE Conference on Computer Vision and Pattern Recognition*, pages 4460–4470, 2019.
- [28] B. Mildenhall, P. P. Srinivasan, M. Tancik, J. T. Barron, R. Ramamoorthi, and R. Ng. Nerf: Representing scenes as neural radiance fields for view synthesis. In *Proceedings of the European Conference on Computer Vision*, 2020.
- [29] B. Mildenhall, P. P. Srinivasan, M. Tancik, J. T. Barron, R. Ramamoorthi, and R. Ng. Nerf: Representing scenes as neural radiance fields for view synthesis. In *Proceedings of the European Conference on Computer Vision*, 2020.

- [30] M. Mirza and S. Osindero. Conditional generative adversarial nets. *arXiv preprint arXiv:1411.1784*, 2014.
- [31] P. Nguyen-Ha, L. Huynh, E. Rahtu, and J. Heikkilä. Predicting Novel Views Using Generative Adversarial Query Network. In *Scandinavian Conference on Image Analysis*, pages 16–27. Springer, 2019.
- [32] T. Nguyen-Phuoc, C. Li, L. Theis, C. Richardt, and Y.-L. Yang. Hologan: Unsupervised learning of 3d representations from natural images. In *Proceedings of the IEEE International Conference on Computer Vision*, pages 7588–7597, 2019.
- [33] K. Olszewski, S. Tulyakov, O. Woodford, H. Li, and L. Luo. Transformable bottleneck networks. In *Proceedings of the IEEE International Conference on Computer Vision*, pages 7648–7657, 2019.
- [34] R. J. Oriez. *Do readers believe what they see?: reader acceptance of image manipulation*. PhD Thesis, University of Missouri–Columbia, 2009.
- [35] E. Park, J. Yang, E. Yumer, D. Ceylan, and A. C. Berg. Transformation-Grounded Image Generation Network for Novel 3D View Synthesis. In *Proceedings of the IEEE Conference on Computer Vision and Pattern Recognition*, pages 3500–3509, 2017.
- [36] J. J. Park, P. Florence, J. Straub, R. Newcombe, and S. Lovegrove. Deepsdf: Learning continuous signed distance functions for shape representation. In *Proceedings of the IEEE Conference on Computer Vision and Pattern Recognition*, pages 165–174, 2019.
- [37] M. S. Pinho, D. A. Bowman, and C. M. Freitas. Cooperative object manipulation in immersive virtual environments: framework and techniques. In *Proceedings of the ACM symposium on Virtual reality software and technology*, pages 171–178, 2002.
- [38] A. Radford, L. Metz, and S. Chintala. Unsupervised representation learning with deep convolutional generative adversarial networks. *arXiv preprint arXiv:1511.06434*, 2015.
- [39] N. Rahaman, A. Baratin, D. Arpit, F. Draxler, M. Lin, F. Hamprecht, Y. Bengio, and A. Courville. On the Spectral Bias of Neural Networks. In *International Conference on Machine Learning*, pages 5301–5310, 2019.
- [40] O. Ronneberger, P. Fischer, and T. Brox. U-net: Convolutional networks for biomedical image segmentation. In *International Conference on Medical image computing and computer-assisted intervention*, pages 234–241. Springer, 2015.
- [41] E. Sabir, J. Cheng, A. Jaiswal, W. AbdAlmageed, I. Masi, and P. Natarajan. Recurrent convolutional strategies for face manipulation detection in videos. *Interfaces (GUI)*, 3:1, 2019.
- [42] S. Saito, Z. Huang, R. Natsume, S. Morishima, A. Kanazawa, and H. Li. Pifu: Pixel-aligned implicit function for high-resolution clothed human digitization. In *Proceedings of the IEEE International Conference on Computer Vision*, pages 2304–2314, 2019.
- [43] S. M. Seitz, B. Curless, J. Diebel, D. Scharstein, and R. Szeliski. A comparison and evaluation of multi-view stereo reconstruction algorithms. In *Proceedings of the 2006 IEEE Computer Society Conference on Computer Vision and Pattern Recognition-Volume 1*, pages 519–528, 2006.
- [44] R. N. Shepard and J. Metzler. Mental rotation of three-dimensional objects. *Science*, 171(3972):701–703, 1971.
- [45] Z. Shu, E. Yumer, S. Hadap, K. Sunkavalli, E. Shechtman, and D. Samaras. Neural face editing with intrinsic image disentangling. In *Proceedings of the IEEE Conference on Computer Vision and Pattern Recognition*, pages 5541–5550, 2017.
- [46] V. Sitzmann, J. Thies, F. Heide, M. Nießner, G. Wetzstein, and M. Zollhöfer. DeepVoxels: Learning Persistent 3D Feature Embeddings. In *Proceedings of the IEEE Conference on Computer Vision and Pattern Recognition*, 2019.

- [47] V. Sitzmann, M. Zollhöfer, and G. Wetzstein. Scene representation networks: Continuous 3D-structure-aware neural scene representations. In *Advances in Neural Information Processing Systems*, pages 1119–1130, 2019.
- [48] E. Smith, S. Fujimoto, A. Romero, and D. Meger. GEOMetrics: Exploiting Geometric Structure for Graph-Encoded Objects. In *International Conference on Machine Learning*, pages 5866–5876, 2019.
- [49] S.-H. Sun, M. Huh, Y.-H. Liao, N. Zhang, and J. J. Lim. Multi-view to Novel View: Synthesizing Novel Views with Self-Learned Confidence. In *Proceedings of the European Conference on Computer Vision*, 2018.
- [50] M. Tatarchenko, A. Dosovitskiy, and T. Brox. Multi-view 3d models from single images with a convolutional network. In *Proceedings of the European Conference on Computer Vision*, pages 322–337. Springer, 2016.
- [51] Y. Tian, X. Peng, L. Zhao, S. Zhang, and D. N. Metaxas. CR-GAN: learning complete representations for multi-view generation. In *Proceedings of the 27th International Joint Conference on Artificial Intelligence*, pages 942–948, 2018.
- [52] H.-Y. F. Tung, R. Cheng, and K. Fragkiadaki. Learning spatial common sense with geometry-aware recurrent networks. In *Proceedings of the IEEE Conference on Computer Vision and Pattern Recognition*, pages 2595–2603, 2019.
- [53] H.-Y. F. Tung, A. W. Harley, W. Seto, and K. Fragkiadaki. Adversarial inverse graphics networks: Learning 2d-to-3d lifting and image-to-image translation from unpaired supervision. In *IEEE International Conference on Computer Vision*, pages 4364–4372. IEEE, 2017.
- [54] N. Wang, Y. Zhang, Z. Li, Y. Fu, W. Liu, and Y.-G. Jiang. Pixel2mesh: Generating 3d mesh models from single rgb images. In *Proceedings of the European Conference on Computer Vision*, pages 52–67, 2018.
- [55] C. Wen, Y. Zhang, Z. Li, and Y. Fu. Pixel2mesh++: Multi-view 3d mesh generation via deformation. In *Proceedings of the IEEE International Conference on Computer Vision*, pages 1042–1051, 2019.
- [56] O. Wiles, G. Gkioxari, R. Szeliski, and J. Johnson. Synsin: End-to-end view synthesis from a single image. In *Proceedings of the IEEE/CVF Conference on Computer Vision and Pattern Recognition*, pages 7467–7477, 2020.
- [57] D. E. Worrall, S. J. Garbin, D. Turmukhambetov, and G. J. Brostow. Interpretable transformations with encoder-decoder networks. In *Proceedings of the IEEE International Conference on Computer Vision*, pages 5726–5735, 2017.
- [58] Q. Xu, W. Wang, D. Ceylan, R. Mech, and U. Neumann. Disn: Deep implicit surface network for high-quality single-view 3d reconstruction. In *Advances in Neural Information Processing Systems*, pages 490–500, 2019.
- [59] X. Xu, Y.-C. Chen, and J. Jia. View Independent Generative Adversarial Network for Novel View Synthesis. In *Proceedings of the IEEE International Conference on Computer Vision*, pages 7791–7800, 2019.
- [60] X. Yan, J. Yang, E. Yumer, Y. Guo, and H. Lee. Perspective transformer nets: Learning single-view 3d object reconstruction without 3d supervision. In *Advances in Neural Information Processing Systems*, pages 1696–1704, 2016.
- [61] G. Yang, X. Huang, Z. Hao, M.-Y. Liu, S. Belongie, and B. Hariharan. Pointflow: 3d point cloud generation with continuous normalizing flows. In *Proceedings of the IEEE International Conference on Computer Vision*, pages 4541–4550, 2019.
- [62] J. Yang, S. E. Reed, M.-H. Yang, and H. Lee. Weakly-supervised disentangling with recurrent transformations for 3d view synthesis. In *Advances in Neural Information Processing Systems*, pages 1099–1107, 2015.

- [63] S. Yao, T. M. Hsu, J.-Y. Zhu, J. Wu, A. Torralba, B. Freeman, and J. Tenenbaum. 3D-aware scene manipulation via inverse graphics. In *Advances in Neural Information Processing Systems*, pages 1887–1898, 2018.
- [64] R. Zhang, P. Isola, A. A. Efros, E. Shechtman, and O. Wang. The unreasonable effectiveness of deep features as a perceptual metric. In *2018 IEEE/CVF Conference on Computer Vision and Pattern Recognition*, pages 586–595. IEEE, 2018.
- [65] T. Zhou, S. Tulsiani, W. Sun, J. Malik, and A. A. Efros. View synthesis by appearance flow. In *Proceedings of the European Conference on Computer Vision*, pages 286–301. Springer, 2016.
- [66] J.-Y. Zhu, T. Park, P. Isola, and A. A. Efros. Unpaired image-to-image translation using cycle-consistent adversarial networks. In *Proceedings of the IEEE International Conference on Computer Vision*, pages 2223–2232, 2017.
- [67] Z. Zhu, P. Luo, X. Wang, and X. Tang. Multi-view perceptron: a deep model for learning face identity and view representations. In *Advances in Neural Information Processing Systems*, pages 217–225, 2014.

Continuous Object Representation Networks: Novel View Synthesis without Target View Supervision

Nicolai Häni Selim Engin Jun-Jee Chao Volkan Isler
{haeni001, engin003, chao0107, isler}@umn.edu
University of Minnesota

Contents

1 Additional Results	1
1.1 Loss function ablations	1
1.2 Additional view synthesis results	2
1.3 Additional results for out-of-domain view synthesis	3
1.4 Additional results on the Basel Face dataset	4
1.5 Additional single view 3D reconstruction results	5
2 Reproducibility	5
2.1 Network Architecture	5
2.2 Implementation details	5
3 Baselines	6
3.1 M2NV:	6
3.2 CVC:	7
3.3 VIGAN:	7
3.4 TBN:	7
3.5 SRN:	7

1 Additional Results

This section presents additional qualitative results of our models for each evaluation scenario presented in the paper.

1.1 Loss function ablations

We use the ShapeNet v2. [1] chair category and train models by ablating parts of the loss function. Due to the long training times per model, we provide ablations only on the chair category. Our transformation chain and 3D feature supervision are shown to be necessary, as they improve the baseline’s performance (Tab. 1). Similarly, performance degrades if the GAN loss or the perceptual loss functions are omitted.

Table 1: **Loss function ablation.** We report mean and standard deviation of the L_1 loss (lower is better), structural similarity (SSIM) index (higher is better) and learned perceptual image patch similarity (LPIPS) (lower is better). The ablation shows the importance of our proposed loss function.

Methods	Chair		
	$L_1(\downarrow)$	SSIM (\uparrow)	LPIPS (\downarrow)
CORN w.o $\mathcal{L}_{\text{trafo}}$	0.211	0.656	0.341
CORN w.o $\mathcal{L}_{\text{GAN/VGG}}$	0.141	0.714	0.216
CORN w.o \mathcal{L}_{GAN}	0.139	0.715	0.208
CORN w.o \mathcal{L}_{3D}	0.133	0.724	0.182
CORN	0.132	0.722	0.180

1.2 Additional view synthesis results

We show additional qualitative results of our model on the ShapeNet v2 [1] cars and chairs categories on the task of transforming a single-source view to a target camera pose.

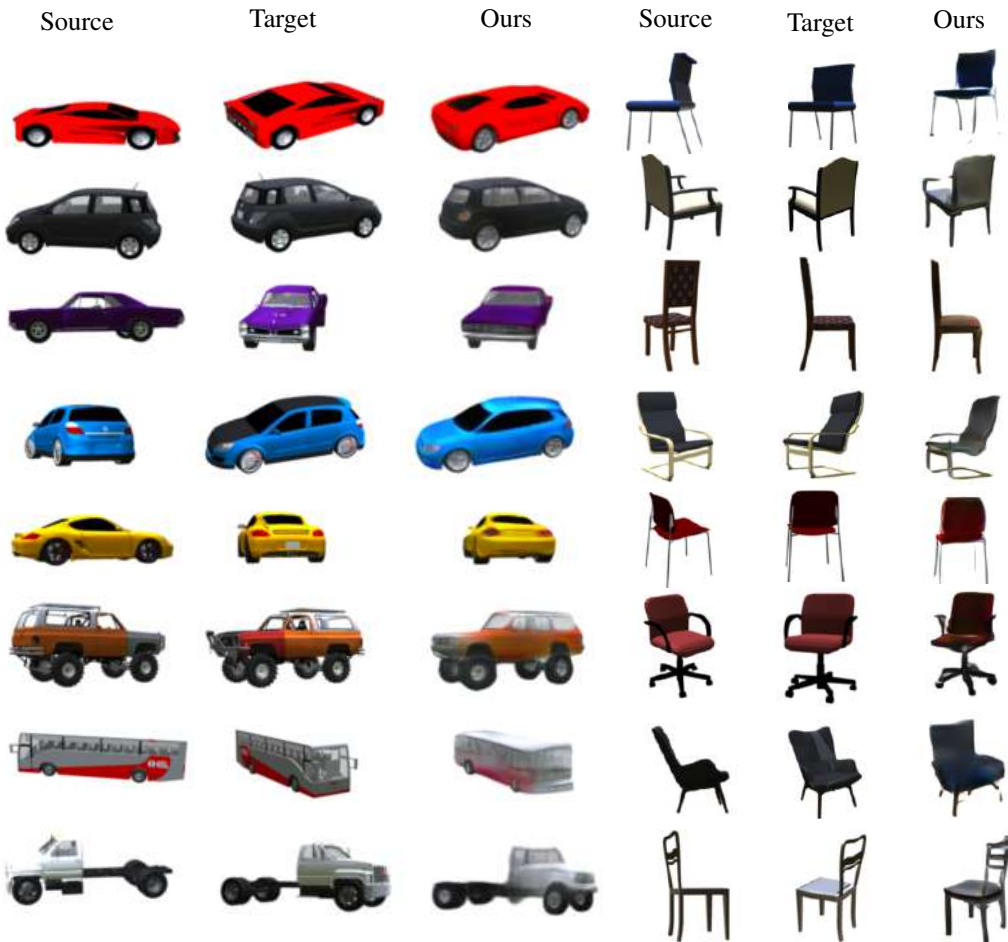


Figure 1: **Additional qualitative results.** Given a single source image and a target camera pose, our method generates fine level details even for unobserved parts of the object. We provide the ground truth view of the objects for reference.

In Fig. 2, we show additional results on the task of creating a sequence of consecutive target views from a single input image.

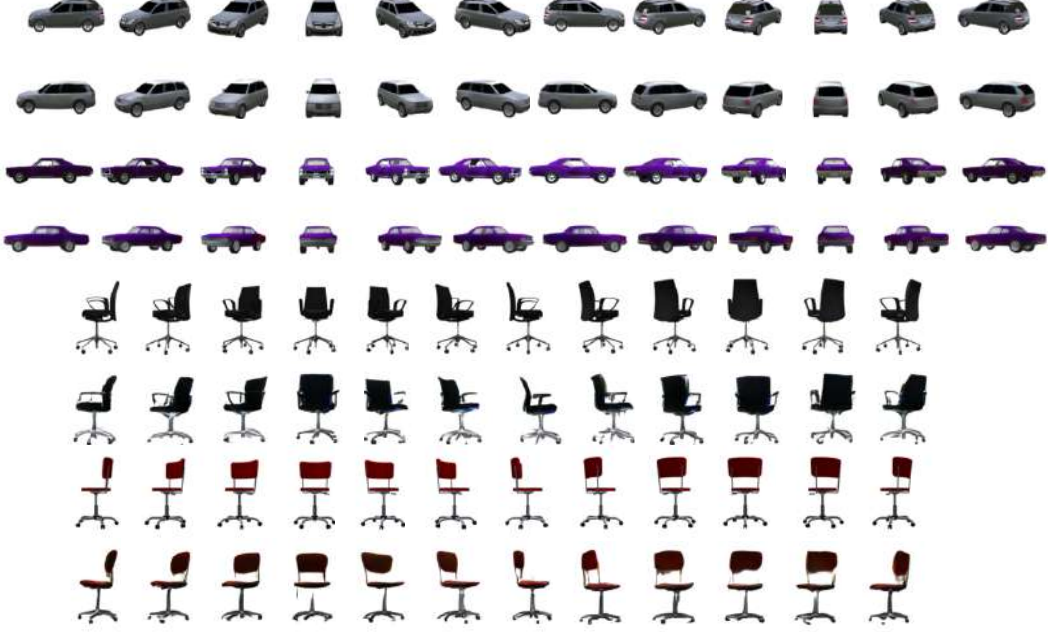


Figure 2: **Additional rotation results.** We used a single image to predict 108 views. Compared to the ground truth image sequence (top row per model) our model (bottom row per model) generates target views with high detail.

1.3 Additional results for out-of-domain view synthesis

In Fig. 3, we show additional results on using our pretrained model on out-of-domain images. We take the model pretrained on the ShapeNet v2 dataset and apply it on images from the Cars [4] dataset without retraining. We observe that the model predicts the structure and appearance correctly; however, the detail degrades compared to the synthetic ShapeNet images. Further, the generated images inhibit the training set's characteristics, with the model being unable to model specularity or all the adequate levels of details.

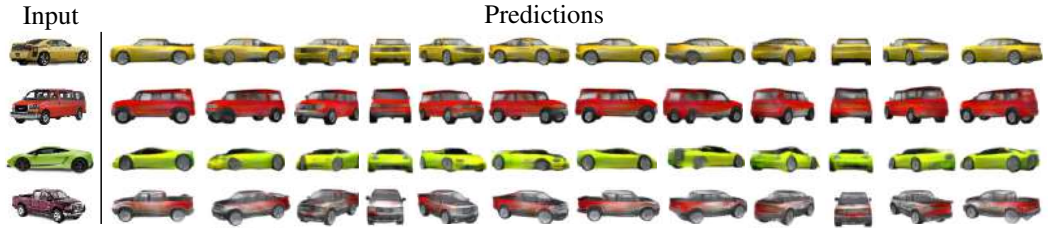


Figure 3: **Additional synthetic → real results.** Given a single image of a real car, we predict 108 novel views. We use our model trained on the synthetic ShapeNet dataset without retraining.

1.4 Additional results on the Basel Face dataset

In Fig. 4, we show additional results on the task of creating a sequence of consecutive target views from a single input image on the Basel Face dataset [3].

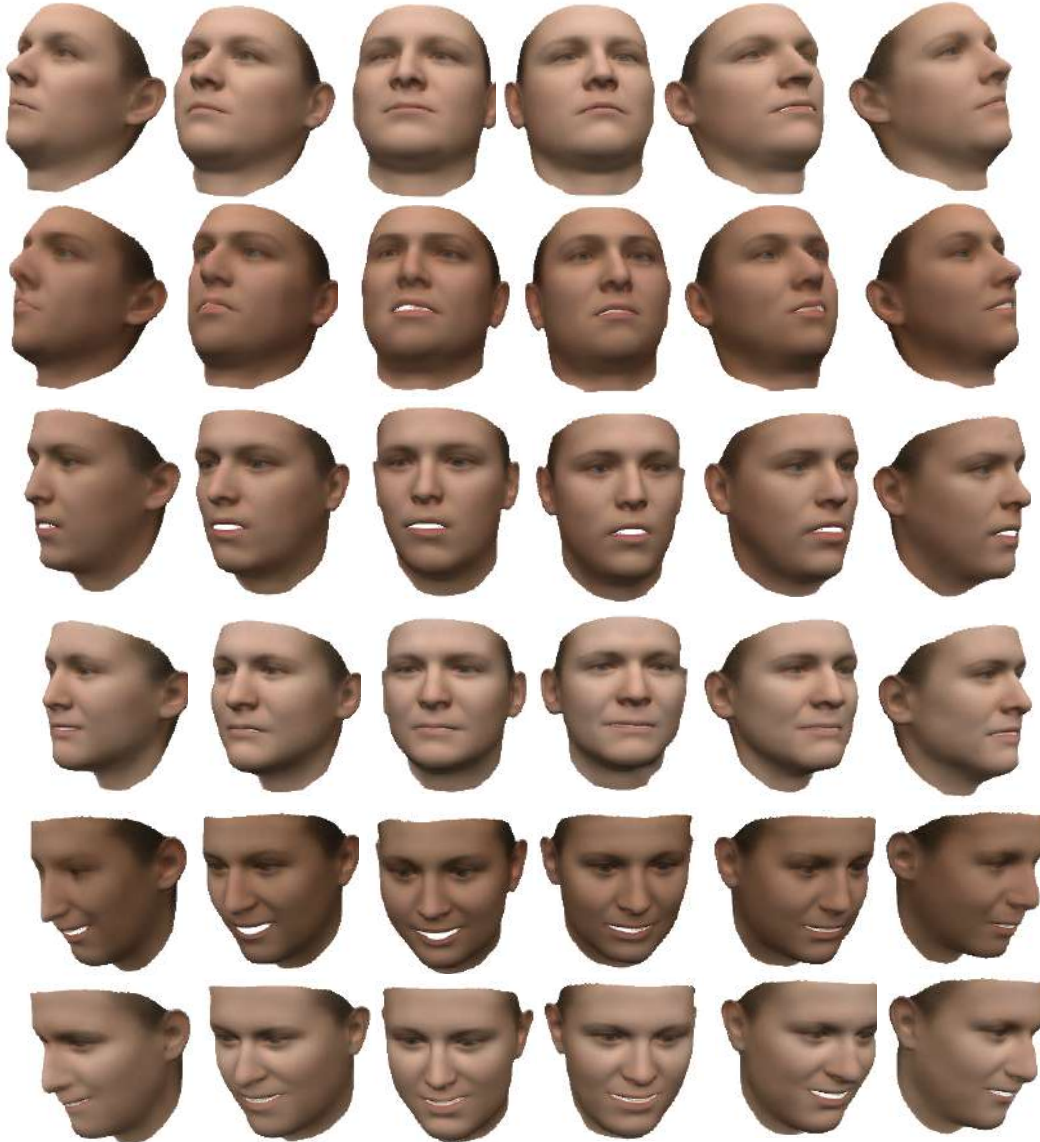


Figure 4: **Additional face rotation results.** We used a single image to predict 33 views.

1.5 Additional single view 3D reconstruction results

In Fig. 5 we show additional examples of using synthesized views for single image 3D reconstruction. We use a single image to predict 15 novel views. We re-project 3D points to each foreground mask to receive occupancy probabilities.

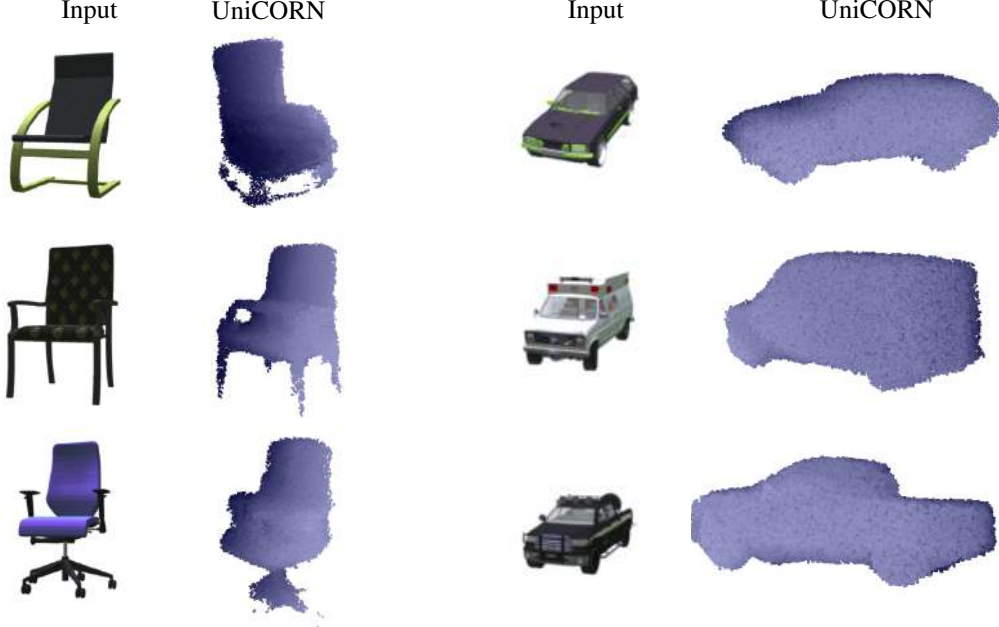


Figure 5: **Additional 3D reconstruction results.** Given a single input image our method can synthesize images from multiple viewpoints to generate the 3D reconstruction of an object.

2 Reproducibility

Here we give more information about the precise architecture used to build our model.

2.1 Network Architecture

Spatial and global object feature network. We use a pretrained ResNet-18 for global and upsample blocks for the local feature extraction. In particular, we use the setup in Fig. 6a.

Continuous function network. We use an MLP for the continuous function network. In particular, we use the setup in Fig. 6b.

Neural renderer. Our neural renderer based on [9] uses disks of radius 2 pixels for splatting and stores 16 points per pixel for z-buffering. Please refer to [9] for additional details.

Refinement network. We use a UNet for the refinement network, containing four down/upsample blocks with skip connections. In particular, we use the setup in Fig. 6c.

2.2 Implementation details

The models are trained with the Adam optimizer, learning rate of 0.0002, and momentum parameters (0, 0.99). Empirically, we found $\lambda_{\text{rec}} = 10$, $\lambda_{\text{3d}} = 1$, $\lambda_{\text{bce}} = 1$, and $\lambda_{\text{gan}} = 0.1$ to lead to good convergence. The models are trained for 45 epochs (chair) and 5 epochs (car). We implemented our models in PyTorch [6]; they take 1-2 days to train on 4 Tesla V100 GPUs. For architectural details please see the supplementary material. Code, data, and model files can be accessed on our project page.

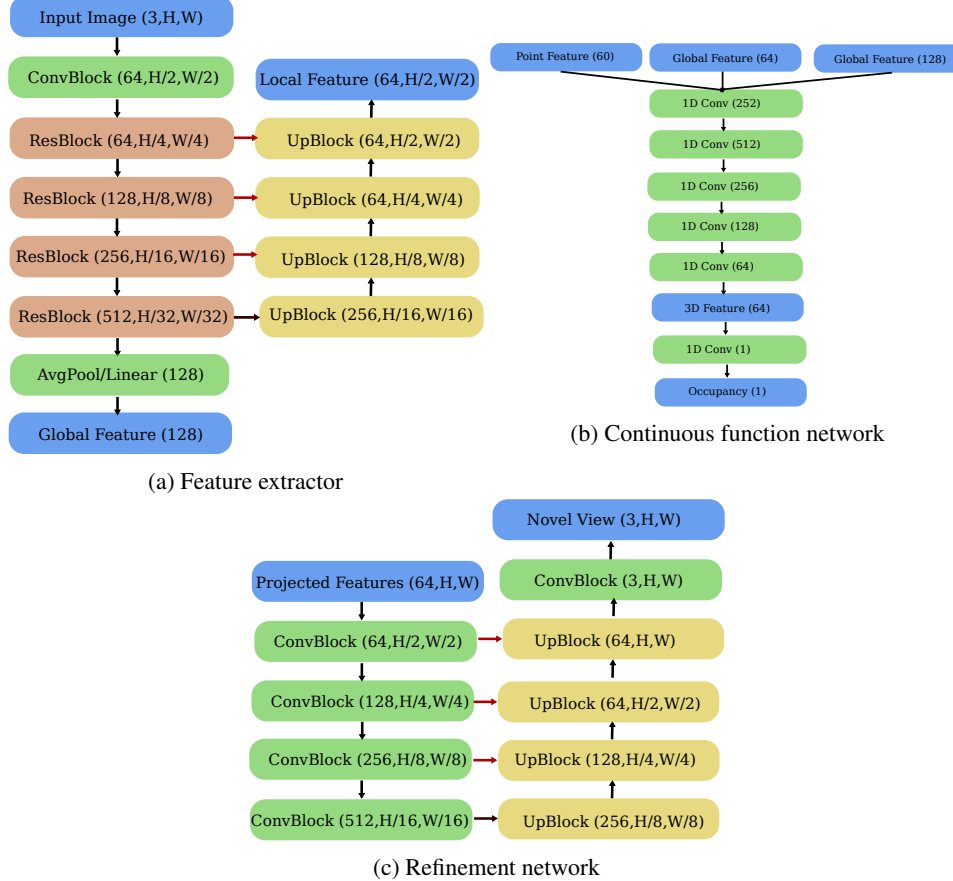


Figure 6: **CORN architecture:** (a) Our feature extractor uses a pretrained ResNet-18 for global feature extraction (left). For local feature extraction (right) we use four upsampling blocks with skip connections (red arrows). (b) Our continuous function network takes as input a position encoding, local features and global features and produces a 3D feature at the given spatial location and an occupancy probability. (c) Our refinement network contains a UNet with four down/upsampling blocks.

3 Baselines

On the task of novel view synthesis, we compare CORN against five current methods that use 2D target view supervision. In our first experiment, we compare our approach against [8, 2, 10, 5], which share a common evaluation protocol. At inference time, the models are presented with a single source image and generate a fixed target view. To compare our method against SRN [7], we use a single image to generate the 3D object representation. From this representation, we synthesize all 108 views and compare them against the ground truth. Note that all these baseline methods have access to the ground truth target images, while our method does not.

3.1 M2NV:

Multi-view to novel view (M2NV) [8] predicts the flow of multiple source images to a single target camera pose. During training, the network predicts each flow map’s confidence scores and aggregates the pixel values in the final target view. At test time, the method can take an arbitrary number of input images.

Training. We use pretrained model weights for the ShapeNet chair and car categories, made available by the authors.

Testing. For novel view synthesis on the test set, the model receives a single input view and generates the requested target view.

3.2 CVC:

Monocular neural image-based rendering with continuous view control (CVC) [2] is another appearance flow method. The approach estimates a 3D latent space that is implicitly rotated to the target camera pose. A decoder uses the rotated latent space to output depth predictions. Using perspective projection, they attain dense per-pixel correspondences, which are used to warp the pixels from the source to the target view.

Training. We use pretrained model weights for the ShapeNet chair and car categories, made available by the authors.

Testing. For novel view synthesis on the test set, the model receives a single input view, and we generate the requested target view. In [2], this method is evaluated for target views that are within $[-40^\circ, 40^\circ]$ rotation from the source image. We evaluate it using the provided models over the entire range of the dataset.

3.3 VIGAN:

View independent generative adversarial networks (VIGAN) [10] predicts novel views by learning a view independent feature map. The network generates novel views in the target camera frame by combining this feature map with the target camera pose. A decoder network synthesizes the final image.

Training. We reimplemented VIGAN and modified the loss functions due to the non-convergence of the original model. We remove all loss functions, except reconstruction, cyclic consistency, pixel losses. The model was trained from scratch on our training dataset for 100,000 iterations (chairs) and 1,000,000 iterations (cars) with the hyperparameters proposed in the original paper.

Testing. For novel view synthesis on the test set, the model receives a single input view, and we generate the requested target view.

3.4 TBN:

Transformable bottleneck networks (TBN) [5] learn a discrete voxel representation from multiple 2D images. The model disentangles viewpoint transformations and the objects' appearance by introducing a transformable bottleneck layer. This bottleneck layer is transformed with arbitrary SO(3) rotations and reprojected to the target camera pose to guarantee multi-view consistency.

Training. We use pretrained model weights for the ShapeNet chair and car categories, made available by the authors. This method is trained using four input images.

Testing. For novel view synthesis on the test set, the model receives a single input view, and we generate the requested target view.

3.5 SRN:

Scene representation networks (SRN) [7] are closely related to our method, learning a continuous scene representation with multi-view consistency.

Training. We use existing models, trained on 50 source images per object.

Testing. We optimize for the latent vectors of objects in our test set until convergence using the provided code and hyperparameter configurations.

References

- [1] A. X. Chang, T. Funkhouser, L. Guibas, P. Hanrahan, Q. Huang, Z. Li, S. Savarese, M. Savva, S. Song, H. Su, and others. Shapenet: An information-rich 3d model repository. *arXiv preprint arXiv:1512.03012*, 2015.

- [2] X. Chen, J. Song, and O. Hilliges. Monocular neural image based rendering with continuous view control. In *Proceedings of the IEEE International Conference on Computer Vision*, pages 4090–4100, 2019.
- [3] T. Gerig, A. Morel-Forster, C. Blumer, B. Egger, M. Luthi, S. Schönborn, and T. Vetter. Morphable face models—an open framework. In *2018 13th IEEE International Conference on Automatic Face & Gesture Recognition*, pages 75–82. IEEE, 2018.
- [4] J. Krause, M. Stark, J. Deng, and L. Fei-Fei. 3d object representations for fine-grained categorization. In *Proceedings of the IEEE international conference on computer vision workshops*, pages 554–561, 2013.
- [5] K. Olszewski, S. Tulyakov, O. Woodford, H. Li, and L. Luo. Transformable bottleneck networks. In *Proceedings of the IEEE International Conference on Computer Vision*, pages 7648–7657, 2019.
- [6] A. Paszke, S. Gross, F. Massa, A. Lerer, J. Bradbury, G. Chanan, T. Killeen, Z. Lin, N. Gimelshein, L. Antiga, A. Desmaison, A. Kopf, E. Yang, Z. DeVito, M. Raison, A. Tejani, S. Chilamkurthy, B. Steiner, L. Fang, J. Bai, and S. Chintala. PyTorch: An Imperative Style, High-Performance Deep Learning Library. In *Advances in Neural Information Processing Systems*, pages 8024–8035. Curran Associates, Inc., 2019.
- [7] V. Sitzmann, M. Zollhöfer, and G. Wetzstein. Scene representation networks: Continuous 3D-structure-aware neural scene representations. In *Advances in Neural Information Processing Systems*, pages 1119–1130, 2019.
- [8] S.-H. Sun, M. Huh, Y.-H. Liao, N. Zhang, and J. J. Lim. Multi-view to Novel View: Synthesizing Novel Views with Self-Learned Confidence. In *Proceedings of the European Conference on Computer Vision*, 2018.
- [9] O. Wiles, G. Gkioxari, R. Szeliski, and J. Johnson. Synsin: End-to-end view synthesis from a single image. In *Proceedings of the IEEE/CVF Conference on Computer Vision and Pattern Recognition*, pages 7467–7477, 2020.
- [10] X. Xu, Y.-C. Chen, and J. Jia. View Independent Generative Adversarial Network for Novel View Synthesis. In *Proceedings of the IEEE International Conference on Computer Vision*, pages 7791–7800, 2019.